SPANDIDOS PUBLICATIONS

MOLECULAR MEDICINE REPORTS 25: 75, 2022

Long non-coding RNA PCAT1 sponges miR-134-3p to regulate PITX2 expression in breast cancer

WEIMING TANG[1], GUANG LU[2], YIN JI[3] and YAN XU[1]

Departments of [1]Clinical Laboratory, [2]General Surgery and [3]Pathology, Liyang People's Hospital, Liyang, Jiangsu 213300, P.R. China

Received November 19, 2020; Accepted September 3, 2021

DOI: 10.3892/mmr.2022.12591

Abstract. Breast cancer (BC) is the most prevalent cancer among women. Long non-coding (lnc)RNAs and microRNAs (miRs) both regulate the expression of key genes in tumorigenesis. The present study aimed to explore the molecular mechanism of the prostate cancer-associated transcript 1 (PCAT1)/miR-134-3p/pituitary homeobox 2 (PITX2) in BC. Reverse transcription-quantitative PCR was performed to examine the expression of miR-134-3p. Cell proliferation, viability, cell cycle, apoptosis and migration were analyzed using Cell Counting Kit-8, colony formation, flow cytometry, wound healing and Transwell assays. Protein expression levels were determined by western blotting. The present study demonstrated that PCAT1 was significantly highly expressed in BC cells. Knockdown of PCAT1 significantly inhibited cell proliferation, migration and invasion, but promoted apoptosis in human BC cell lines. The results of the dual-luciferase assay showed that PCAT1 targeted miR-134-3p, and PITX2 was a potential target of miR-134-3p. Western blotting results demonstrated that PCAT1 knockdown significantly reduced the protein expression levels of anti-apoptotic protein Bcl-2, and significantly upregulated the protein expression levels of proapoptotic proteins, Bax, cleaved caspase-3 and cleaved caspase-9. Furthermore, the effect of a miR-134-3p inhibitor on BC progression was rescued by the knockdown of PITX2 in cells transfected with short hairpin RNA-lncRNA PCAT1. To conclude, the results of the present study indicated that the PCAT1/miR-134-3p/PITX2 axis could be a promising therapeutic target in BC treatment.

Introduction

Breast cancer (BC) is a leading cause of cancer-related mortality in women worldwide and remains the most common malignancy among younger patients (1-3). Although treatments have improved, including chemotherapy and radiotherapy, BC prognoses remain poor (4). Therefore, it is important to investigate the molecular mechanisms of BC growth and metastasis to discover novel molecular targets for BC treatment (5).

Long non-coding (lnc)RNAs are defined as non-coding transcripts that are >200 nucleotides in length. Dysregulated lncRNA expression has be observed in numerous types of cancer, which suggests that aberrant lncRNA expression may be a major contributor to tumorigenesis (6-9). lncRNAs also regulate various biological processes, including cell proliferation, apoptosis, differentiation, migration and invasion in the cancer microenvironment (9-11), and therefore provide new opportunities for cancer diagnosis and treatment (9,12). For example, lncRNA RUSC1-AS1 promotes the progression of BC through mediating cyclin-dependent kinase inhibitor 1 and kruppel-like factor 2 (13). Overexpression of lncRNA HOTAIR has been shown to promote the development of retinoblastoma via the miR-613/c-met axis, which modulates the epithelial-mesenchymal transition in retinoblastoma (14). Furthermore, lncRNA in non-homologous end joining pathway 1 may promote BC growth by regulating BC cell metastasis and increasing the expression of epithelial-mesenchymal transition-related markers (15).

lncRNA prostate cancer-associated transcript 1 (PCAT1) was first discovered in 2011 as a prostate-specific regulator of cell proliferation in prostate cancer (16). Recent studies have indicated that PCAT1 serves a role in numerous types of cancer (16-18). It has also been reported that PCAT1 promotes epithelial ovarian cancer by mediating the expression of cyclin D1/CDK4 (17). Furthermore, PCAT1 knockdown may reduce the expression of cyclin B1 and CDC2 kinase activity, inhibiting the growth of esophageal squamous cell carcinoma (ESCC) by sponging miR-326 (19). Therefore, the aim of the present study was to explore the function and molecular mechanism of lncRNA PCAT1/microRNAs (miRNAs/miRs)-134-3p/pituitary homeobox 2 (PITX2) in BC.

Materials and methods

Tissue specimens. This study involved 30 patients who underwent BC resection at Liyang People's Hospital (Liyang, China) between March 2019 and March 2020. All patients were newly diagnosed with primary BC. Patients <18 or >75 years of age,

Correspondence to: Dr Yan Xu, Department of Clinical Laboratory, Liyang People's Hospital, 157 Tianmu Road, Liyang, Jiangsu 213300, P.R. China
E-mail: xuyan216012600@163.com

Key words: long non-coding RNA prostate cancer-associated transcript 1, microRNA-134-3p, pituitary homeobox 2, breast cancer

who presented with first distant metastasis, combined with other malignancies, or who received neoadjuvant therapy were excluded from the present study. Tumor and matched adjacent normal tissues were collected and stored in liquid nitrogen. The present study was approved by the Ethics Committee of Liyang People's Hospital (approval no. 2018024), and were conducted in accordance with the Declaration of Helsinki. Written informed consent was obtained from all participants prior to the study.

Cell culture and transfection. Human BC cell lines (MDA-MB-231, SKBr-3, MCF-7 and ZR-75-30) and the normal human mammary epithelial MCF10A cell line were purchased from the American Type Culture Collection. MDA-MB-231, MCF10A, SKBr-3 and MCF-7 were cultured in DMEM (Thermo Fisher Scientific, Inc.) supplemented with 10% fetal bovine serum (FBS; Thermo Fisher Scientific, Inc.), 100 U/ml penicillin and 100 μg/ml streptomycin and incubated at 37˚C in an atmosphere containing 5% CO_2. ZR-75-30 cells were cultured in RPMI-1640 medium (Thermo Fisher Scientific, Inc.) supplemented with 10% FBS, 100 U/ml penicillin and 100 μg/ml streptomycin and incubated at 37˚C in an atmosphere containing 5% CO_2.

For cell transfection, short hairpin RNAs (shRNAs) targeting lncRNA PCAT1 (sh-PCAT1), PITX2 (sh-PITX2) and the corresponding sh-negative control (NC) were subcloned into the GV248 (hU6-MCS-UbiquitinEGFP-IRES-puromycin) vector (Shanghai GeneChem Co., Ltd.). The following sequences were used: sh-PCAT1, 5'-ATACATAAGACCATGGAAAT-3'; sh-PITX2, 5'-GATGCAATGATGTTTCTGAAA-3'; and sh-NC, 5'-TTCTCCGAACGTGTCACGT-3'. miR-134-3p mimic, miR-134-3p inhibitor and their corresponding NCs (NC mimic and NC inhibitor) were purchased from Thermo Fisher Scientific, Inc.

The sequences were as follows: miR-134-3p mimic, 5'-CCUGUGGGCCACCUAGUCACCAA-3'; miR-134-3p inhibitor, 5'-CCUGUGGGCCACCUAGUCACCAA-3'; NC mimic, 5'-UUCUCCGAACGUGUCACGUTT-3'; and NC inhibitor, 5' UCACAACCUCCUAGAAAGAGU AGA 3'. For plasmid or miRNA mimic/inhibitor transfection, SKBR-3 and MCF-7 cells were seeded in 6-well plates at a density of $1x10^6$ cells/well and cultured to 80% confluence. Plasmids (1 μg) or miRNA mimic/inhibitor (20 nm) were transfected into cells using Lipofectamine® 2000 (Invitrogen; Thermo Fisher Scientific, Inc.). Cells were then cultured at 37˚C for 24 h, and transfection efficiency was assessed. Subsequent experiments were performed 48 h post-transfection.

Reverse transcription-quantitative PCR (RT-qPCR). Total RNA was extracted from BC and adjacent normal tissue samples or cells (MCF10A, MDA-MB-231, SKBr-3, MCF-7 and ZR-75-30). To detect the expression levels of miR-134-3p, the miRNeasy Kit (Shanghai Yeasen Biotechnology Co., Ltd.) was used to extract total RNA. Total RNA was reverse transcribed using the miScript II RT Kit (Qiagen, Inc.) into complementary DNA (cDNA) according to the manufacturer's protocol. qPCR reaction systems were prepared using the miScript SYBR Green PCR Kit (Qiagen, Inc.) with U6 as the internal reference gene. To detect the mRNA expression levels, total RNA was extracted using TRIzol® reagent (Takara Bio, Inc.). Total RNA was reverse transcribed into cDNA using the PrimeScript™ II 1st Strand cDNA Synthesis Kit (Takara Biotechnology Co., Ltd.) according to the manufacturer's protocol. All PCR reactions were carried out using an ABI 7500 System (Applied Biosystems; Thermo Fisher Scientific, Inc.). GAPDH and U6 were used as the internal reference genes. The following primers were used for qPCR: PCAT1 forward (F), 5'-GCTGGCATTGGTCAACATAAC-3' and reverse (R), 5'-GTGAATATGGCGGATGAGGAA-3'; miR-134-3p F, 5'-CTGTGGGCCACCTAGTCACCAA-3' and R, 5'-GCTGTCAACGATACGCTACCTA-3'; PITX2 F, 5'-GGCCGCCGCTTCTTACA-3' and R, 5'-CACTGGCGA TTTGGTTCTGATTT-3'; U6 F, 5'-GTGATCACTCCCTGCC TGAG-3' and R, 5'-GGACTTCACTGGACCAGACG-3'; and GAPDH F, 5'-CCGCATCTTCTTGTGCAGTG-3' and R, 5'-CCCAATACGGCCAAATCCGT-3'. The thermocycling conditions were as follows: 10 min at 95˚C for 1 cycle, followed by denaturation at 95˚C for 30 sec, annealing at 56˚C for 1 min, and final extension at 72˚C for 30 sec for 40 cycles. Relative gene expression was calculated using the $2^{-\Delta\Delta Cq}$ method (20) and were normalized to either GAPDH or U6 levels.

Cell proliferation assay. The proliferation rates of SKBr-3 and MCF-7 cells were analyzed using the Cell Counting Kit-8 (CCK-8) assay (Dojindo Laboratories, Inc.) according to the manufacturer's instructions. Cells were seeded into 96-well plates at a density of ~4,000 cells/well. Cells were then incubated for 24, 48 and 72 h. Subsequently, 10 μl CCK-8 reagent was added to each well. The plates were incubated at 37˚C for 2 h. The optical density was measured at 450 nm using a ultraviolet spectrophotometer (Thermo Fisher Scientific, Inc.).

Wound healing assay. The migratory abilities of SKBr-3 and MCF-7 cells were analyzed using wound healing assays. Transfected cells ($5x10^5$ cells/well) were inoculated into 6-well plates and incubated in serum-free medium. Subsequently, the confluent cell monolayer (95-100%) was scratched using a 200 μl pipette tip. Cell migration was observed and quantified at 0 and 48 h. Migrated cells were counted in three randomly selected fields using an IX70 inverted optical microscope (magnification, x100; Olympus Corporation). Cell migration was calculated according to the following formula: Cell migration (%) = (width at 0 h - width at 48 h) / width at 0 h x100.

Transwell assay. The migration and invasion of SKBr-3 and MCF-7 cells were analyzed using Transwell assays. The upper chamber was filled with serum-free DMEM containing $5x10^4$ cells, and the lower chamber was filled with DMEM containing 10% FBS. Following incubation for 24 h at 37˚C, cells in the lower chamber were collected and stained with 0.5% crystal violet for 20 min at room temperature. Stained cells were counted using an IX70 inverted optical microscope (magnification, x100; Olympus Corporation). The invasion assay was carried out using the aforementioned Transwell assay protocol, but the upper chamber was precoated with Matrigel (37˚C for 30 min).

Colony formation assay. The colony forming ability of SKBr-3 and MCF-7 cells was assessed using a colony formation assay. The SKBr-3 or MCF-7 cells were seeded into 6-well plates

at a density of $1x10^3$ cells/well. Colonies were formed for 10 days at room temperature and then the culture medium was removed. Following which, the colonies were washed with PBS three times and fixed with methyl alcohol for 10 min at room temperature and stained with 0.5% crystal violet solution for a further 10 min at room temperature. After washing with water, the colonies were imaged and counted under a light microscope (magnification, x10; Olympus Corporation).

Cell cycle analysis. Flow cytometry was used for SKBr-3 and MCF-7 cells ($1x10^5$) cycle analysis. Cells were collected and centrifuged at 100 x g at room temperature for 5-10 min. Cells were digested using trypsin and fixed in 70% ethanol and incubated at 4˚C for 1 h. Subsequently, the cells were incubated with 25 μg/ml PI, 25 μl/ml RNase A and Triton X-100 for 30 min at 4˚C. The cell cycle results were detected using a flow cytometer (FACSCalibur; BD Biosciences) and analyzed with FlowJo software (version 10.9; FlowJo LLC).

Flow cytometry. Flow cytometry was employed for early and late apoptosis analysis, which was completed using an Annexin V-FITC kit (Thermo Fisher Scientific, Inc.) according to the manufacturer's protocol. SKBr-3 and MCF-7 cells ($1x10^5$) were collected and centrifuged at 100 x g at room temperature for 5-10 min. Cells were first stained with 5 μl Annexin V-FITC and 5 μl PI simultaneously at 4˚C for 15 min in the dark. Cell apoptosis was detected using a flow cytometer (FACSCalibur; BD Biosciences). The apoptosis results were analyzed with FlowJo software (version 10.9; FlowJo LLC).

Western blotting. Total protein from SKBr-3 and MCF-7 cells after transfection was extracted using RIPA buffer (Invitrogen; Thermo Fisher Scientific, Inc.), followed by quantification using the BCA Assay Kit (Santa Cruz Biotechnology, Inc.). Then, 25 μg protein/lane was separated by SDS-PAGE on an 8-12% gel. The separated proteins were transferred onto a 0.22-μm PVDF membrane and blocked in Tris-buffered saline with 1% Tween-20 and 5% non-fat milk for 1 h at room temperature. Subsequently, the membranes were incubated overnight at 4˚C with primary antibodies (all from Abcam) targeted against: Anti-Bax (1:1,000; cat. no. ab32503), anti-Bcl-2 (1:1,000; cat. no. ab32124), anti-cleaved caspase-3 (1:500; cat. no. ab32042), anti-cleaved caspase-9 (1:500; cat. no. ab2324), anti-cyclooxygenase 2 (Cox-2; 1:1,000; cat. no. ab179800), anti-MMP-2 (1:1,000; cat. no. ab92536), anti-MMP-9 (1:1,000; cat. no. ab76003), anti-PITX2 (1:1,000; cat. no. ab221142) and anti-GAPDH (1:2,000; cat. no. ab181602). Following which, membranes were incubated with a HRP-conjugated anti-rabbit secondary antibody (1:10,000; cat. no. ab6721; Abcam) for 2 h at room temperature. Protein bands were visualized via enhanced chemiluminescence (Pierce; Thermo Fisher Scientific, Inc.) and were semi-quantified using ImageJ software (version 1.42; National Institutes of Health).

Dual-luciferase reporter assay. The starBase database (version 2.0; http://starbase.sysu.edu.cn/starbase2/) was used to predict the potential miRNA and miR-134-3p target genes. Wild-type (WT) and mutant (Mut) PCAT1 3' untranslated regions (3'UTRs) were integrated into the pGL3 vector (Promega Corporation) to synthesize pGL3-PCAT1-WT and pGL3-PCAT1-Mut. The WT and Mut 3'UTRs of PITX2 were also integrated into the luciferase reporter plasmid psiCHECK-2 (Promega Corporation) to synthesize psiCHECK-2-PITX2-WT and psiCHECK-2-PITX2-Mut. SKBr-3 and MCF-7 cells at $5x10^4$ cells/well in 24-well plates were co-transfected with WT or Mut PCAT1 3'UTR or Mut PITX2 3'UTR reporter plasmids and miR-134-3p mimic or mimic NC using Lipofectamine 2000 at 37˚C for 48 h. Luciferase activity was detected using the Dual-Luciferase Reporter Assay System (Promega Corp.). Firefly luciferase activity was normalized to *Renilla* luciferase activity.

Statistical analysis. All presented data were obtained from at least three independent experiments. All of the data were carried out using GraphPad Prism 10.0.(GraphPad Software, Inc.). Data are presented as the mean ± standard deviation (SD). Statistical comparisons were determined using unpaired/paired Student's t-tests, Mann-Whitney U test or one-way ANOVA followed by Bonferroni's post hoc test. Pearson's correlation coefficient was used to analyze the correlation between the expression levels of PCAT1 and miR-134-3p in clinical BC samples. $P<0.05$ was considered to indicate a statistically significant difference.

Results

Knockdown of PCAT1 inhibits BC cell proliferation. The expression patterns of PCAT1 were determined to investigate its biological function in human BC cell lines. PCAT1 expression levels were evaluated in 30 paired human BC specimens and normal adjacent tissues. The results demonstrated that PCAT1 expression levels were significantly higher in BC specimens compared with those in normal adjacent tissues (Fig. 1A). Furthermore, PCAT1 expression levels in multiple human BC cell lines were upregulated compared with those in MCF10A cells, especially in SKBr-3 and MCF-7 cells (Fig. 1B). Therefore, to further investigate the role of PCAT1 in human BC, sh-PCAT1 and its scrambled control (sh-NC) were transfected into SKBr-3 and MCF-7 cells. The knockdown efficiency of sh-PCAT1 in SKBr-3 and MCF-7 cells was validated using RT-qPCR analysis. The results demonstrated that sh-PCAT1 significantly decreased PCAT1 expression levels compared with sh-NC (Fig. 1C). CCK-8 and colony formation assays demonstrated that PCAT1 knockdown significantly inhibited the proliferation of SKBr-3 and MCF-7 cells compared with the sh-NC group (Fig. 1D and E). Cell proliferation is closely connected with the cell cycle. Therefore, the effects of PCAT1 knockdown on the cell cycle in SKBr-3 and MCF-7 cells were investigated. The results demonstrated that PCAT1 knockdown significantly induced cell cycle arrest in the G_1 phase compared with in the sh-NC group (Fig. 1F). At the molecular level, PCAT1 knockdown resulted in significantly downregulated cyclin D1 and significantly upregulated p21 protein expression levels compared with in the sh-NC group (Fig. 1G). Flow cytometry revealed that PCAT1 knockdown significantly promoted the apoptosis of SKBr-3 and MCF-7 cells compared with in the sh-NC group (Fig. 1H). Furthermore, the protein expression levels of apoptosis-related proteins were examined by western blotting. The results demonstrated that PCAT1 knockdown significantly reduced the protein expression levels of antiapoptotic protein Bcl-2, and significantly upregulated

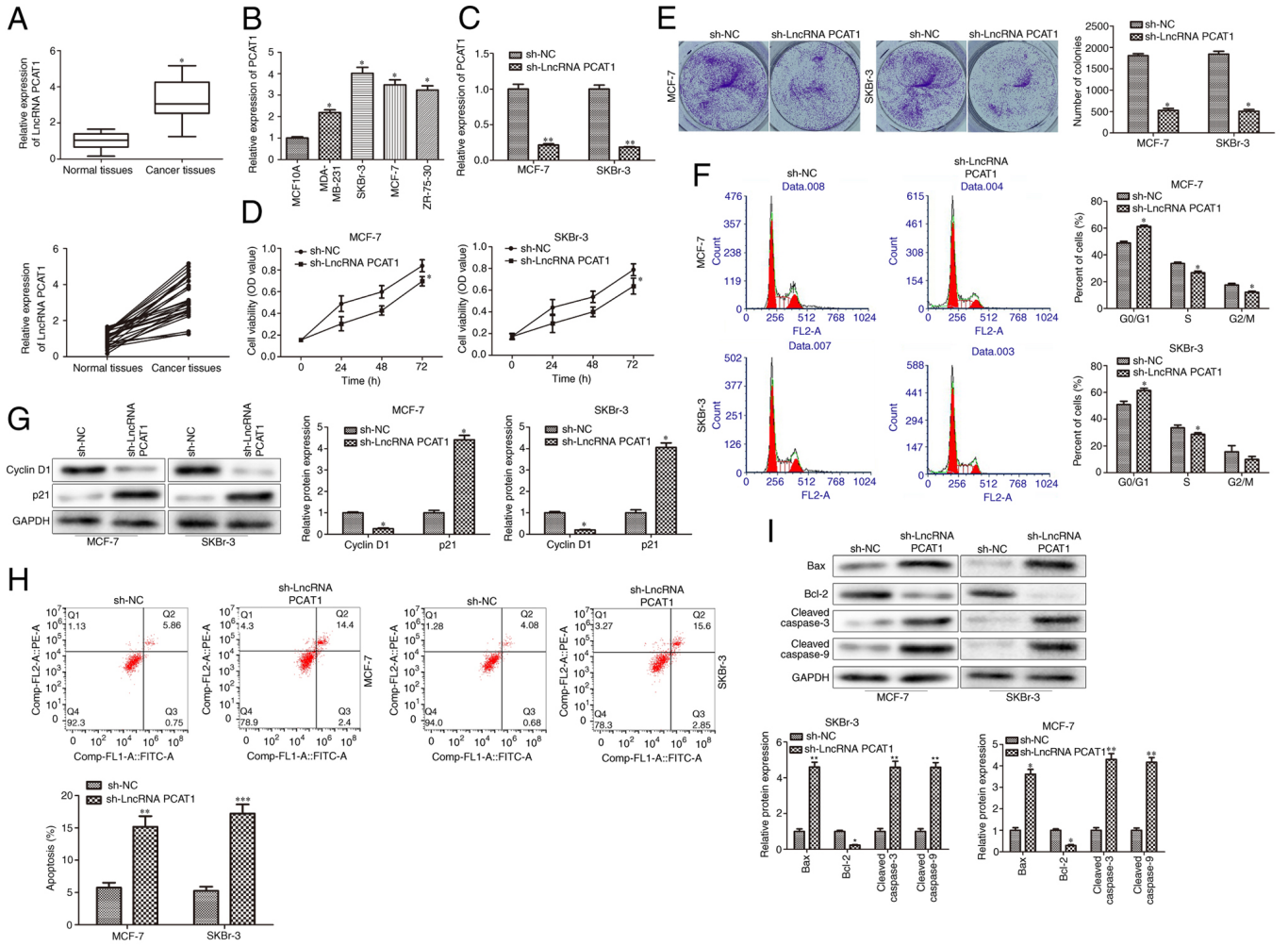

Figure 1. PCAT1 is highly expressed in BC cells and its knockdown inhibits BC cell proliferation. (A) RT-qPCR was performed to determine PCAT1 expression levels in BC specimens and normal adjacent tissues. Data are presented as the mean ± SD. *P<0.05 vs. normal adjacent tissues. n=30. (B) RT-qPCR was performed to determine PCAT1 expression levels in BC cell lines (MDA-MB-231, SKBr-3 and MCF-7 and ZR-75-30) and the human mammary epithelial MCF10A cell line. Data are presented as the mean ± SD. *P<0.05 vs. MCF10A. n=3. BC SKBr-3 and MCF-7 cell lines were transfected with sh-PCAT1. (C) RT-qPCR was performed to detect the knockdown efficiency of sh-PCAT1. (D) Cell Counting Kit-8 assays were performed to determine cell proliferation at 24, 28 and 72 h in SKBr-3 and MCF-7 cells. (E) Colony formation assays were performed to demonstrate cell proliferation in SKBr-3 and MCF-7 cells. (F) Flow cytometry was used to analyze the cell cycle. (G) Western blotting was performed to determine cyclin D1 and p21 protein expression levels. (H) Flow cytometry was used to analyze the apoptotic rate. (I) Western blotting was performed to determine the protein expression levels of apoptosis-associated proteins, Bax, Bcl-2, cleaved caspase-3 and cleaved caspase-9. Data are presented as the mean ± SD. *P<0.05, **P<0.01 and ***P<0.001 vs. sh-NC. n=3. PCAT1, prostate cancer-associated transcript 1; BC, breast cancer; RT-qPCR, reverse transcription-quantitative PCR; lncRNA, long non-coding RNA; sh, short hairpin; NC, negative control; PE, phycoerythrin.

the protein expression levels of proapoptotic proteins, Bax, cleaved caspase-3 and cleaved caspase-9 in SKBr-3 and MCF-7 cells (Fig. 1I). Overall, these results indicated that knockdown of PCAT1 may inhibit proliferation and promote the apoptosis of human BC cells.

Knockdown of PCAT1 inhibits the migration and invasion of BC cells. Wound healing and Transwell assays demonstrated that the migration and invasion of SKBr-3 and MCF-7 cells were significantly reduced in cells transfected with sh-PCAT1 compared with sh-NC (Fig. 2A and B). Western blotting also revealed that the protein expression levels of migration- and invasion-related proteins, Cox-2, MMP-2 and MMP-9, were significantly downregulated by sh-PCAT1 in SKBr-3 and MCF-7 cells compared with in the sh-NC group (Fig. 2C). Overall, these results indicated that sh-PCAT1 may inhibit the migration and invasion of human BC cells.

PCAT1 targets miR-134-3p in human BC cells. Subsequently, the molecular mechanism of PCAT1 in BC was investigated. Cytoplasmic and nuclear RNA were extracted from SKBr-3 and MCF-7 cells. The RT-qPCR results demonstrated that PCAT1 was significantly more highly expressed in the cytoplasmic fraction compared with in the nuclear fraction (Fig. 3A). Therefore, the starBase database was used to predict the potential miRNA PCAT1 interacted with, identifying miR-134-3p as a potential target (Fig. 3B). To evaluate the interaction between miR-134-3p and PCAT1, the dual-luciferase reporter assay was performed. The results demonstrated a significant decrease in luciferase activity in cells co-transfected with PCAT1-WT and

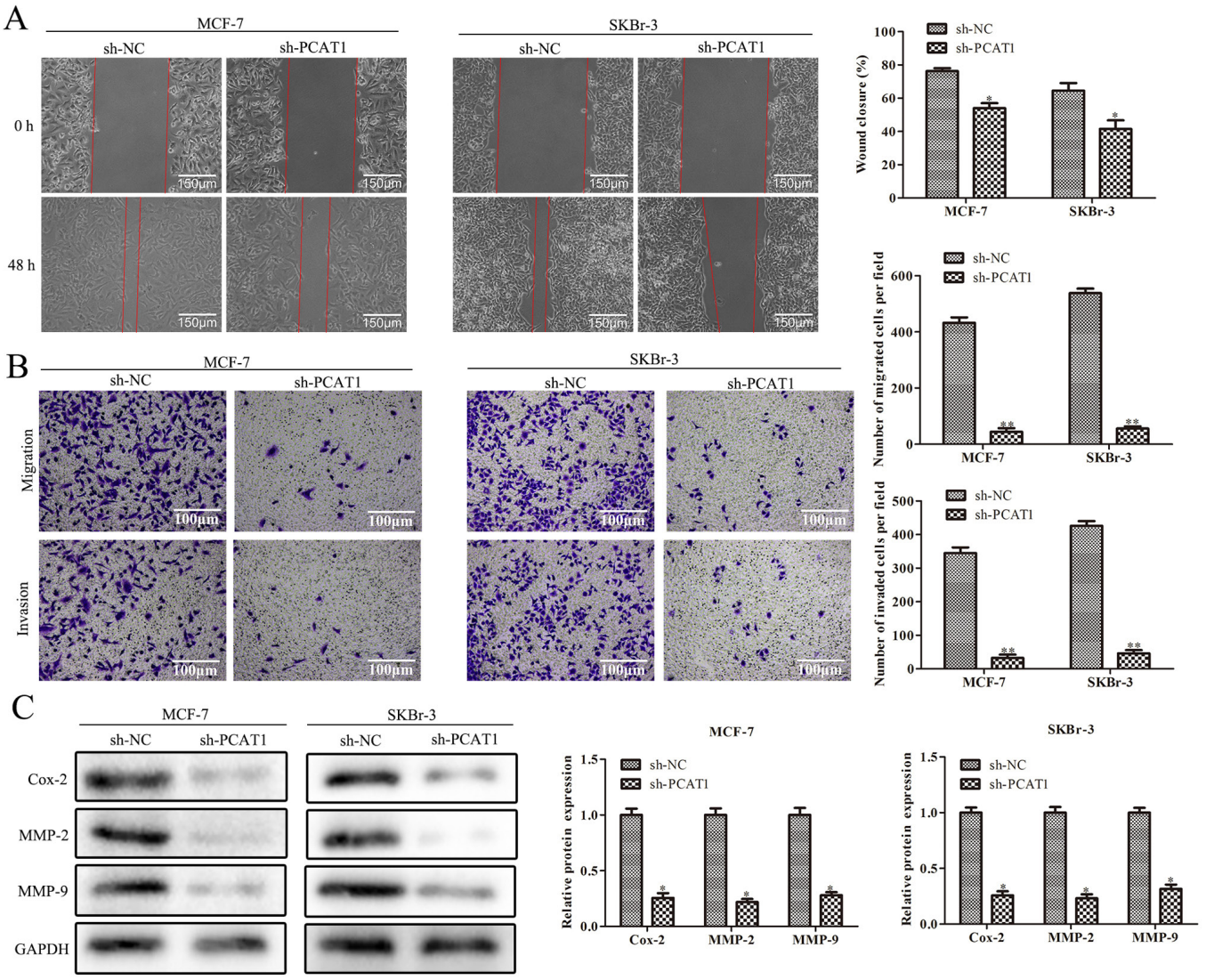

Figure 2. Knockdown of PCAT1 inhibits migration and invasion of breast cancer cells. SKBr-3 and MCF-7 cell lines were transfected with sh-PCAT1. (A) Wound healing and (B) Transwell assays were performed to assess the migration and invasion of SKBr-3 and MCF-7 cells. (C) Western blotting was performed to determine the protein expression levels of the migration and invasion-related proteins expression levels, Cox-2, MMP-2 and MMP-9. Data are presented as the mean ± SD. *P<0.05 and **P<0.01 vs. sh-NC. n=3. PCAT1, prostate cancer-associated transcript 1; sh, short hairpin; Cox-2, cyclooxygenase 2; NC, negative control.

miR-134-3p mimic compared with the NC-mimic (Fig. 3C). However, no significant difference was observed in luciferase activity between the miR-134-3p mimic group and NC mimic group when the putative binding sites were mutated (Fig. 3C). Furthermore, miR-134-3p expression levels in multiple human BC cell lines were significantly downregulated compared with those in MCF10A cells (Fig. 3D). miR-134-3p expression levels were upregulated when SKBr-3 and MCF-7 cells were transfected with sh-PCAT1 compared with sh-NC (Fig. 3E). These results indicated that PCAT1 may function as a sponge for miR-134-3p in SKBr-3 and MCF-7 cells.

miR-134-3p overexpression inhibits cell proliferation, migration and invasion, and promotes apoptosis in human BC cells. In order to investigate the biological function of miR-134-3p in BC progression, miR-134-3p mimic and NC mimic were transfected into SKBr-3 and MCF-7 cells. RT-qPCR was performed to confirm the overexpression efficiency of miR-134-3p mimic in SKBr-3 and MCF-7 cells. Compared with the NC mimic, miR-134-3p expression levels were significantly upregulated by miR-134-3p mimic transfection (Fig. 4A). CCK-8 and colony formation assays demonstrated that miR-134-3p mimic significantly inhibited the proliferation of SKBr-3 and MCF-7 cells compared with the NC mimic (Fig. 4B and C). Furthermore, flow cytometry elucidated that miR-134-3p overexpression significantly promoted cell apoptosis in SKBr-3 and MCF-7 cells compared with the NC mimic (Fig. 4D). The Transwell assay further demonstrated that migration and invasion were significantly reduced in SKBr-3 and MCF-7 cells transfected with miR-134-3p mimic compared with the NC mimic (Fig. 4E). These data indicated that miR-134-3p overexpression may inhibit cell proliferation, migration and invasion but promote apoptosis in human BC cells.

PITX2 is a potential target of miR-134-3p. To explore the regulatory mechanism of miR-134-3p in BC progression,

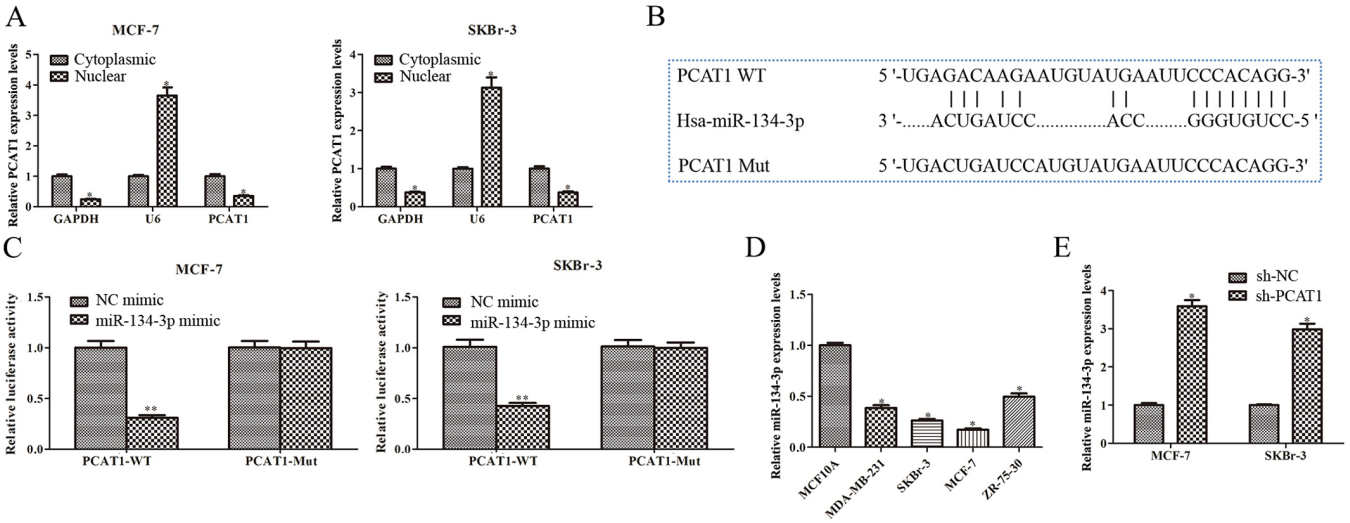

Figure 3. PCAT1 functions as a sponge for miR-134-3p in human BC cells. (A) RT-qPCR was performed to determine PCAT1 expression levels in cell cytoplasmic and nuclear fractions. *P<0.05 vs. Cytoplasmic. (B) Bioinformatics analysis using starBase was performed to predict the binding site between PCAT1 and miR-134-3p. (C) Dual-luciferase reporter assays were used to detect the luciferase activity of PCAT1-WT in SKBr-3 and MCF-7 cells. **P<0.01 vs. NC mimic. SKBr-3 and MCF-7 cells were transfected with miR-134-3p mimic. (D) RT-qPCR was performed to determine miR-134-3p expression levels in BC cell lines (MDA-MB-231, SKBr-3 and MCF-7 and ZR-75-30) and the human mammary epithelial MCF10A cell line. *P<0.01 vs. MCF10A. (E) RT-qPCR was performed to determine miR-134-3p expression levels in SKBr-3 and MCF-7 cells transfected with sh-PCAT1. *P<0.01 vs. sh-NC. Data are presented as the mean ± SD. n=3. PCAT1, prostate cancer-associated transcript 1; miR, microRNA; BC, breast cancer; sh, short hairpin; RT-qPCR, reverse transcription-quantitative PCR; NC, negative control; WT, wild-type; Mut, mutant.

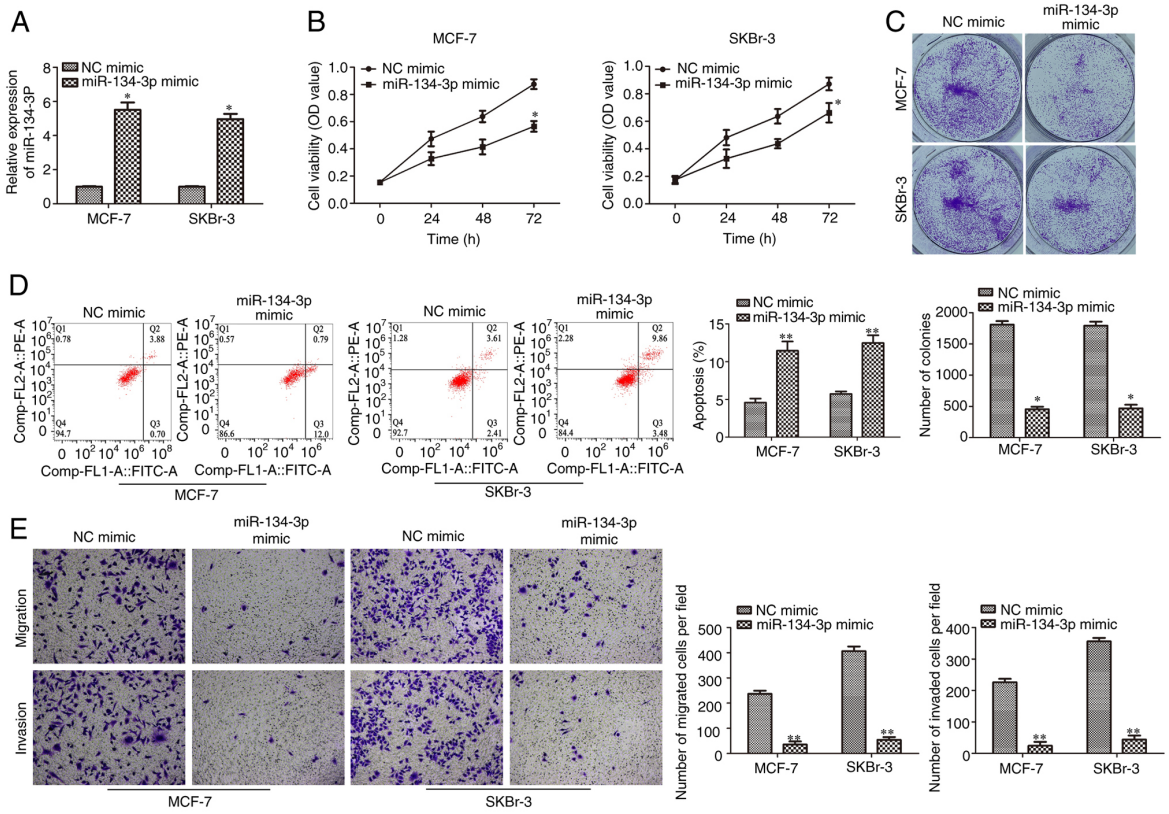

Figure 4. Overexpression of miR-134-3p inhibits cell proliferation, migration and invasion but promotes apoptosis in human breast cancer cells. SKBr-3 and MCF-7 cells were transfected with miR-134-3p mimics. (A) Reverse transcription-quantitative PCR was performed to determine miR-134-3p expression levels. (B) Cell Counting Kit-8 and (C) colony formation assays were performed to assess cell proliferation. (D) Flow cytometry was performed to determine the apoptotic rate. (E) Transwell assays were performed to assess cell migration and invasion abilities. *P<0.05 and **P<0.01 vs. NC mimic. Data are presented as the mean ± SD. n=3. miR, microRNA; NC, negative control; PE, phycoerythrin.

the starBase database was used to predict miR-134-3p target genes and identified PITX2 as a potential target (Fig. 5A). The dual-luciferase reporter assay was used to determine the interaction between miR-134-3p and PITX2. The results demonstrated

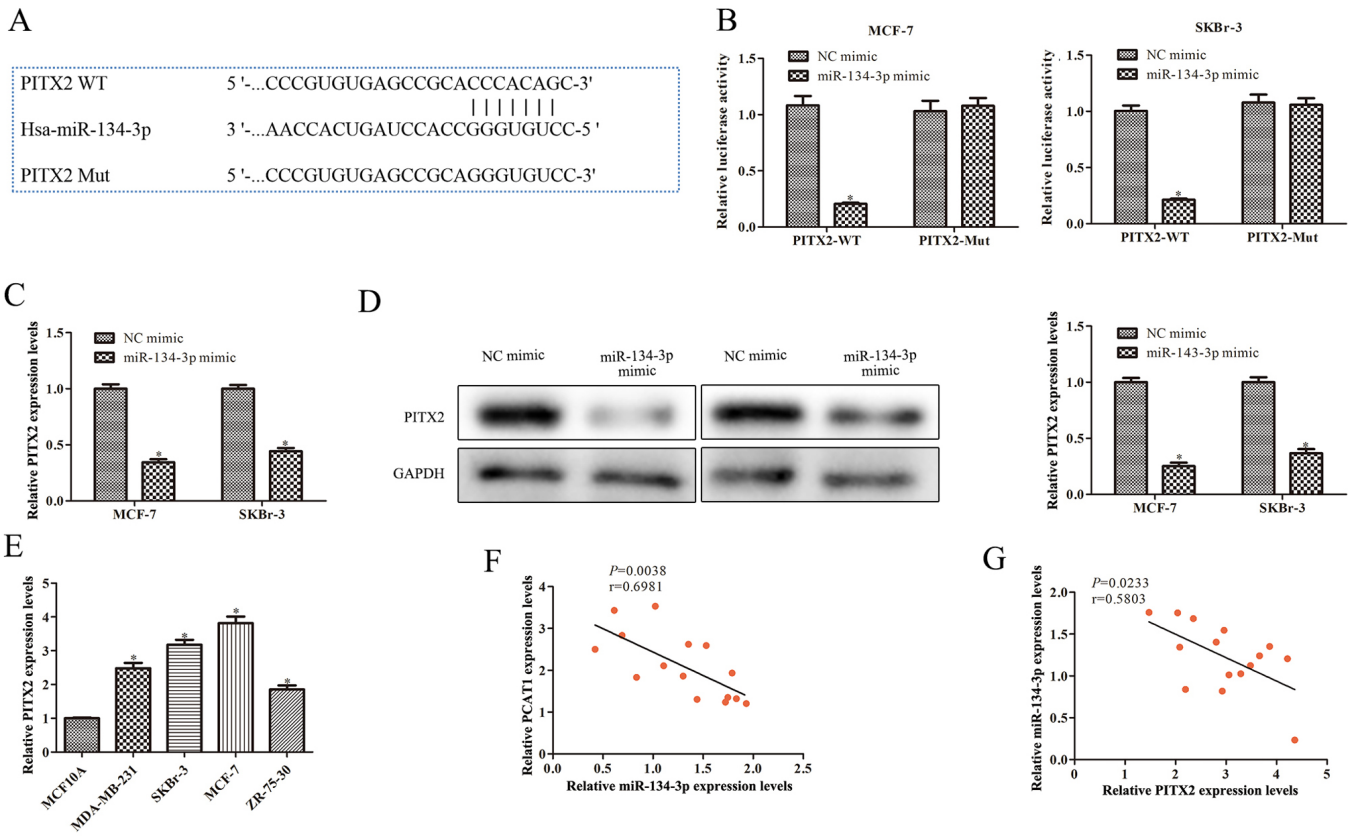

Figure 5. PCAT1 regulates the expression of PITX2 via miR-134-3p. (A) Bioinformatics analysis using starBase predicted the binding site between PITX2 and miR-134-3p. (B) Dual-luciferase reporter assays were performed following co-transfection of SKBr-3 and MCF-7 cells with the luciferase reporter plasmid, containing WT or Mut forms of the PITX2 3'untranslated region, and NC mimic or miR-134-3p mimic. (C) RT-qPCR was performed to determine PITX2 mRNA expression levels in SKBr-3 and MCF-7 cells transfected with miR-134-3p mimic. (D) Western blotting was performed to analyze PITX2 protein expression levels. *P<0.05 vs. NC mimic. (E) RT-qPCR was performed to determine PITX2 mRNA expression levels in human BC cell lines and the human mammary epithelial MCF10A cell line. *P<0.05 vs. MCF10A cells. Correlation coefficient analysis demonstrated a negative correlation between (F) PCAT1 and miR-134-3p expression levels and between (G) miR-134-3p and PITX2 expression levels in clinical BC samples. Data are presented as the mean ± SD. n=3. PCAT1, prostate cancer-associated transcript 1; PITX2, pituitary homeobox 2; miR, microRNA; WT, wild-type; Mut, mutant; NC, negative control; RT-qPCR, reverse transcription-quantitative PCR; BC, breast cancer.

that luciferase activity was significantly reduced when the cells were co-transfected with PITX2-WT and miR-134-3p mimics. However, there was no significant difference in luciferase activity of PITX2-Mut between cells transfected with miR-134-3p mimic or NC mimic (Fig. 5B). To further analyze the association between PITX2 and miR-134-3p, RT-qPCR and western blotting were used. The results demonstrated that PITX2 mRNA and protein expression levels were significantly decreased by miR-134-3p mimic in SKBr-3 and MCF-7 cells compared with the NC mimic (Fig. 5C and D). Furthermore, PITX2 mRNA expression levels were significantly increased in BC cells (MDA-MB-231, ZR-75-30, SKBr-3 and MCF-7) compared with those in MCF10A cells (Fig. 5E). Pearson's correlation coefficient analysis demonstrated a negative correlation between PCAT1 and miR-134-3p expression levels, and between miR-134-3p and PITX2 expression levels in clinical BC samples (Fig. 5F and G). These results indicated that PITX2 may be a downstream target gene of miR-134-3p and that PCAT1 may regulate PITX2 expression via miR-134-3p.

sh-PITX2 rescues the function of the miR-134-3p inhibitor in human BC cells. Rescue experiments were performed to investigate the functions of PCAT1, miR-134-3p and PITX2 in human BC cells. Transfection efficiency is shown in Fig. S1A and B. miR-134-3p expression levels were significantly downregulated when cells were co-transfected with miR-134-3p inhibitor and sh-PCAT1, in SKBr-3 and MCF-7 cells, compared with NC inhibitor and sh-PCAT1. PITX2 mRNA expression levels were also significantly downregulated when cells were co-transfected with sh-PITX2 and sh-PCAT1 in SKBr-3 and MCF-7 cells, compared with sh-NC and sh-PCAT1 (Fig. 6A). Colony formation and CCK-8 assays demonstrated PITX2 knockdown significantly reversed the effect of miR-134-3p inhibition on the proliferation of SKBr-3 and MCF-7 cells transfected with sh-PCAT1 compared with the miR-134-3p inhibitor + sh-NC group (Fig. 6B and C). Subsequently, an apoptotic assay was performed via flow cytometry. Compared with miR-134-3p inhibitor + sh-NC, the results demonstrated that sh-PITX2 significantly reversed the suppressive effects of miR-134-3p inhibitor on cell apoptosis in SKBr-3 and MCF-7 cells following PCAT1 knockdown (Fig. 6D). Moreover, Transwell assays demonstrated that sh-PITX2 significantly reversed miR-134-3p inhibitor-enhanced cell migration and invasion of PCAT1-knockdown SKBr-3 and MCF-7 cells compared with the miR-134-3p inhibitor + sh-NC group (Fig. 6E). Overall, these results demonstrated that sh-PITX2

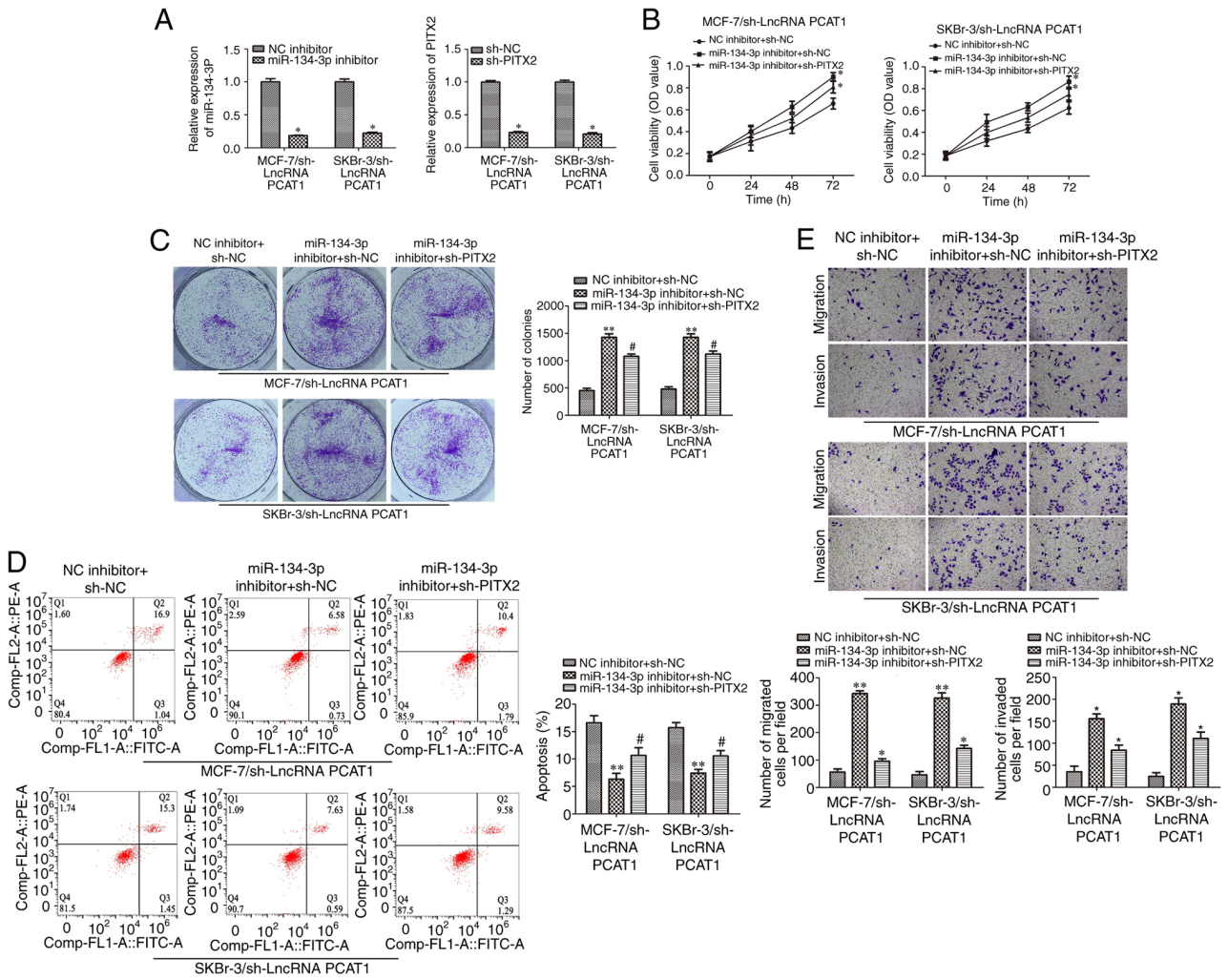

Figure 6. sh-PITX2 reverses the effects of the miR-134-3p inhibitor on human breast cancer cells. sh-PCAT1 was transfected into SKBr-3 and MCF-7 cells with miR-134-3p inhibitor and/or sh-PITX2. (A) Reverse transcription-quantitative PCR was performed to determine miR-134-3p and PITX2 expression levels in SKBr-3 and MCF-7 cells transfected with miR-134-3p inhibitor or sh-PITX2. *P<0.05 vs. NC inhibitor; *P<0.05 vs. sh-NC. (B) Cell Counting Kit-8 assays were used to detect cell proliferation of SKBr-3 and MCF-7 cells transfected with miR-134-3p inhibitor and/or sh-PITX2. *P<0.05 vs. NC inhibitor + sh-NC; $^{\#}$P<0.05 vs. miR-134-3p inhibitor + shPITX2. (C) Colony formation assays were performed to analyze the cell proliferation of SKBr-3 and MCF-7 cells transfected with miR-134-3p inhibitors and/or sh-PITX2. (D) Flow cytometry was performed to analyze the apoptotic rate of SKBr-3 and MCF-7 cells transfected with miR-134-3p inhibitors and/or sh-PITX2. (E) Transwell assays for migration and invasion were performed using SKBr-3 and MCF-7 cells transfected with miR-134-3p inhibitors and/or sh-PITX2. *P<0.05, **P<0.01 vs. NC inhibitor + sh-NC; $^{\#}$P<0.05 vs. miR-134-3p inhibitor + sh-PITX2. Data are presented as the mean ± SD. n=3. sh, short hairpin; PITX2, pituitary homeobox 2; miR, microRNA; PCAT1, prostate cancer-associated transcript 1; NC, negative control; PE, phycoerythrin.

could reverse the function of the miR-134-3p inhibitor on SKBr-3 and MCF-7 cells, suggesting that PITX2 serves a role in BC tumorigenesis via the miRNA 'sponge' mechanism.

Discussion

BC is one of the most common types of cancer in women (21,22), with ~500,000 BC-related deaths each year. Traditional therapeutic approaches, such as surgery and chemotherapy, rarely completely cure BC and the treatment process is painful; in addition, most patients will develop recurrence following treatment (23). Therefore, the identification of novel treatment strategies is important and urgently needed. Previous studies have reported that lncRNAs are crucial regulators involved in cancer-related gene expression and cancer development (8,17,24). Consequently, lncRNAs may become new potential therapeutic targets in clinical applications (25).

lncRNA PCAT1 was first discovered to be upregulated in patients with prostate cancer, whereby it was demonstrated to promote prostate cell proliferation (17). Previous studies have reported that PCAT1 knockdown may inhibit malignant phenotypes in numerous types of human cancer, including gastric cancer, lung cancer and hepatocellular carcinoma (26-28). lncRNA PCAT1 has been shown to be upregulated in human non-small cell lung cancer (NSCLC), and knockdown of PCAT1 can markedly suppress cell growth by inducing cell cycle arrest and apoptosis in NSCLC cells (28). In the present study, PCAT1 expression levels were found to be significantly upregulated in BC cell lines in comparison with the non-tumorigenic epithelial MCF10A cell line. Downregulation of PCAT1 expression levels was significantly associated with the inhibition of BC cell proliferation and an increase in apoptosis-related protein expression levels. These data demonstrated that PCAT1 possibly promotes the progression of BC.

lncRNAs are considered to play an important regulatory role in carcinogenesis and cancer development. They regulate the interaction between proteins and genes as a scaffold or guide, and act as a bait for binding proteins or miRNA (29). The interaction between lncRNA and miRNA functional networks has attracted much attention (30). lncRNAs can function by sponging miRNAs to regulate the expression of specific genes (19) and can therefore affect cancer progression. For example, lncRNA nuclear paraspeckle assembly transcript 1 has been reported to be upregulated in BC and to inhibit the activation of the miR-133b/translocase of inner mitochondrial membrane 17A axis (29). lncRNA PCAT1 was also shown to promote ESCC cell proliferation by sponging miR-326 and may therefore serve as a non-invasive biomarker for ESCC (19). Increasing evidence has indicated that miR-134 is essential for human carcinoma, including lung, BC and colorectal cancer, and that it participates in tumor cell proliferation, apoptosis, invasion and metastasis (31-35). miR-134-3p, as a member of the miR-134 family, has been reported to have a significant regulatory role in non-small cell lung cancer proliferation and invasion (31). Although the downstream mechanism of miR-134-3p in cancer progression has been extensively studied, to the best of our knowledge, the upstream regulatory mechanism of miR-134-3p has not been elucidated until now. In the present study, miR-134-3p was identified as a target of PCAT1 and miR-134-3p expression levels were significantly downregulated in BC cell lines, which was negatively associated with PCAT1 expression levels. Moreover, miR-134-3p mimic significantly inhibited cell proliferation, migration and invasion, but significantly increased the apoptotic rate of BC cell lines. Together, these results demonstrated that PCAT1 may regulate BC progression by sponging miR-134-3p.

PITX2 was predicted to be a possible target of miR-134-3p by bioinformatics analysis, but the mechanisms of miR-134-3p and PITX2 in BC remain unclear. Previous studies have highlighted the association of PITX2 with the progression of numerous types of human cancer, including gonadotroph tumors and colorectal cancer (36-38). In the present study, PITX2 was experimentally confirmed as a target of miR-134-3p. PITX2 mRNA expression levels were negatively associated with miR-134-3p expression levels. Moreover, sh-PITX2 partially significantly reduced the lncRNA PCAT1/miR-134-3p knockdown-mediated effects on cell proliferation, migration, invasion and apoptosis in BC cell lines.

Overall, these findings demonstrated that PCAT1 may induce the downregulation of PITX2 expression levels in BC progression possibly via the upregulation of miR-134-3p expression levels. Each of the three molecules in the PCAT1/miR-134-3p/PITX2 axis may become a novel therapeutic target for the treatment of BC, which is of crucial significance for the clinical prevention and diagnosis of BC. However, the detailed mechanisms of how PITX2 functions in BC requires further investigation.

Acknowledgements

Not applicable.

Funding

No funding was received.

Availability of data and materials

All data generated or analyzed during this study are included in this published article.

Authors' contributions

YX, WT, GL and YJ contributed to the conception and design of the present study, and were responsible for the acquisition, analysis and interpretation of the data. YX and WT confirm the authenticity of all the raw data. YX and WT drafted and critically revised the work for important intellectual content. YX gave final approval of the version to be published. YX and WT agree to be accountable for all aspects of the work in ensuring that questions related to the accuracy or integrity of any part of the work are appropriately investigated and resolved. All authors read and approved the final manuscript.

Ethics approval and consent to participate

The experimental protocol of the present study was in accordance with the Declaration of Helsinki and was approved by the Ethics Committee of the Liyang People's Hospital (Liyang, China; approval no. 2018024). Written informed consent was obtained from all patients.

Patient consent for publication

Not applicable.

Competing interests

The authors declare that they have no competing interests.

References

1. Lu G, Li Y, Ma Y, Lu J, Chen Y, Jiang Q, Qin Q, Zhao L, Huang Q, Luo Z, *et al*: Long noncoding RNA LINC00511 contributes to breast cancer tumourigenesis and stemness by inducing the miR-185-3p/E2F1/Nanog axis. J Exp Clin Cancer Res 37: 289, 2018.
2. Xia W, Liu Y, Cheng T, Xu T, Dong M and Hu X: Down-regulated lncRNA SBF2-AS1 inhibits tumorigenesis and progression of breast cancer by sponging microRNA-143 and repressing RRS1. J Exp Clin Cancer Res 39: 18, 2020.
3. Corey B, Smania MA, Spotts H and Andersen M: Young Women With Breast Cancer: Treatment, Care, and Nursing Implications. Clin J Oncol Nurs 24: 139-147, 2020.
4. Guo Q, Lv S, Wang B, Li Y, Cha N, Zhao R, Bao W and Jia B: Long non-coding RNA PRNCR1 has an oncogenic role in breast cancer. Exp Ther Med 18: 4547-4554, 2019.
5. Zhou Y, Meng X, Chen S, Li W, Li D, Singer R and Gu W: IMP1 regulates UCA1-mediated cell invasion through facilitating UCA1 decay and decreasing the sponge effect of UCA1 for miR-122-5p. Breast Cancer Res 20: 32, 2018.
6. Huang Z, Zhou JK, Peng Y, He W and Huang C: The role of long noncoding RNAs in hepatocellular carcinoma. Mol Cancer 19: 77, 2020.
7. Gugnoni M and Ciarrocchi A: Long Noncoding RNA and Epithelial Mesenchymal Transition in Cancer. Int J Mol Sci 20: 20, 2019.
8. Guo Q, Zhang Q, Lu L and Xu Y: Long noncoding RNA RUSC1-AS1 promotes tumorigenesis in cervical cancer by acting as a competing endogenous RNA of microRNA-744 and consequently increasing Bcl-2 expression. Cell Cycle 19: 1222-1235, 2020.
9. Schmitt AM and Chang HY: Long Noncoding RNAs in Cancer Pathways. Cancer Cell 29: 452-463, 2016.

10. Fan S, Yang Z, Ke Z, Huang K, Liu N, Fang X and Wang K: Downregulation of the long non-coding RNA TUG1 is associated with cell proliferation, migration, and invasion in breast cancer. Biomed Pharmacother 95: 1636-1643, 2017.
11. Zeng H, Wang J, Chen T, Zhang K, Chen J, Wang L, Li H, Tuluhong D, Li J and Wang S: Downregulation of long non-coding RNA Opa interacting protein 5-antisense RNA 1 inhibits breast cancer progression by targeting sex-determining region Y-box 2 by microRNA-129-5p upregulation. Cancer Sci 110: 289-302, 2019.
12. Davalos V and Esteller M: Disruption of Long Noncoding RNAs Targets Cancer Hallmark Pathways in Lung Tumorigenesis. Cancer Res 79: 3028-3030, 2019.
13. Hu CC, Liang YW, Hu JL, Liu LF, Liang JW and Wang R: lncRNA RUSC1-AS1 promotes the proliferation of breast cancer cells by epigenetic silence of KLF2 and CDKN1A. Eur Rev Med Pharmacol Sci 23: 6602-6611, 2019.
14. Yang G, Fu Y, Lu X, Wang M, Dong H and Li Q: lncRNA HOTAIR/miR-613/c-met axis modulated epithelial-mesenchymal transition of retinoblastoma cells. J Cell Mol Med 22: 5083-5096, 2018.
15. Liang Y, Li Y, Song X, Zhang N, Sang Y, Zhang H, Liu Y, Chen B, Zhao W, Wang L, *et al*: Long noncoding RNA LINP1 acts as an oncogene and promotes chemoresistance in breast cancer. Cancer Biol Ther 19: 120-131, 2018.
16. Shang Z, Yu J, Sun L, Tian J, Zhu S, Zhang B, Dong Q, Jiang N, Flores-Morales A, Chang C, *et al*: lncRNA PCAT1 activates AKT and NF-κB signaling in castration-resistant prostate cancer by regulating the PHLPP/FKBP51/IKKα complex. Nucleic Acids Res 47: 4211-4225, 2019.
17. Ding C, Wei R, Rodríguez RA and Del Mar Requena Mullor M: lncRNA PCAT-1 plays an oncogenic role in epithelial ovarian cancer by modulating cyclinD1/CDK4 expression. Int J Clin Exp Pathol 12: 2148-2156, 2019.
18. Zhen Q, Gao LN, Wang RF, Chu WW, Zhang YX, Zhao XJ, Lv BL and Liu JB: lncRNA PCAT-1 promotes tumour growth and chemoresistance of oesophageal cancer to cisplatin. Cell Biochem Funct 36: 27-33, 2018.
19. Huang L, Wang Y, Chen J, Wang Y, Zhao Y, Wang Y, Ma Y, Chen X, Liu W, Li Z, *et al*: Long noncoding RNA PCAT1, a novel serum-based biomarker, enhances cell growth by sponging miR-326 in oesophageal squamous cell carcinoma. Cell Death Dis 10: 513, 2019.
20. Livak KJ and Schmittgen TD: Analysis of relative gene expression data using real-time quantitative PCR and the 2(-Delta Delta C(T)) Method. Methods 25: 402-408, 2001.
21. Bray F, Ferlay J, Soerjomataram I, Siegel RL, Torre LA and Jemal A: Global cancer statistics 2018: GLOBOCAN estimates of incidence and mortality worldwide for 36 cancers in 185 countries. CA Cancer J Clin 68: 394-424, 2018.
22. Feng RM, Zong YN, Cao SM and Xu RH: Current cancer situation in China: Good or bad news from the 2018 Global Cancer Statistics? Cancer Commun (Lond) 39: 22, 2019.
23. Tang R, Wu JC, Zheng LM, Li ZR, Zhou KL, Zhang ZS, Xu DF and Chen C: Long noncoding RNA RUSC1-AS-N indicates poor prognosis and increases cell viability in hepatocellular carcinoma. Eur Rev Med Pharmacol Sci 22: 388-396, 2018.
24. Shen WJ, Zhang F, Zhao X and Xu J: lncRNAs and Esophageal Squamous Cell Carcinoma - Implications for Pathogenesis and Drug Development. J Cancer 7: 1258-1264, 2016.
25. Hou J, Wang L, Wu Q, Zheng G, Long H, Wu H, Zhou C, Guo T, Zhong T, Wang L, *et al*: Long noncoding RNA H19 upregulates vascular endothelial growth factor A to enhance mesenchymal stem cells survival and angiogenic capacity by inhibiting miR-199a-5p. Stem Cell Res Ther 9: 109, 2018.
26. Bi M, Yu H, Huang B and Tang C: Long non-coding RNA PCAT-1 over-expression promotes proliferation and metastasis in gastric cancer cells through regulating CDKN1A. Gene 626: 337-343, 2017.
27. Wen J, Xu J, Sun Q, Xing C and Yin W: Upregulation of long non coding RNA PCAT-1 contributes to cell proliferation, migration and apoptosis in hepatocellular carcinoma. Mol Med Rep 13: 4481-4486, 2016.
28. Li J, Li Y, Wang B, Ma Y and Chen P: lncRNA-PCAT-1 promotes non-small cell lung cancer progression by regulating miR-149-5p/LRIG2 axis. J Cell Biochem: Dec 19, 2018 (Epub ahead of print). doi: 10.1002/jcb.28046.
29. Li X, Deng S, Pang X, Song Y, Luo S, Jin L and Pan Y: lncRNA NEAT1 Silenced miR-133b Promotes Migration and Invasion of Breast Cancer Cells. Int J Mol Sci 20: 20, 2019.
30. Chen L, Zhou Y and Li H: lncRNA, miRNA and lncRNA-miRNA interaction in viral infection. Virus Res 257: 25-32, 2018.
31. Qin Q, Wei F, Zhang J and Li B: miR-134 suppresses the migration and invasion of non small cell lung cancer by targeting ITGB1. Oncol Rep 37: 823-830, 2017.
32. Qin Q, Wei F, Zhang J, Wang X and Li B: miR-134 inhibits non-small cell lung cancer growth by targeting the epidermal growth factor receptor. J Cell Mol Med 20: 1974-1983, 2016.
33. Xie Y, Song J, Zong Q, Wang A, Yang Y, Liu F and Meng X: Decreased Expression of MIR-134 and its Clinical Significance in Human Colorectal Cancer. Hepatogastroenterology 62: 615-619, 2015.
34. Zhang J, Ma Y, Wang S, Chen F and Gu Y: C/EBPα inhibits proliferation of breast cancer cells via a novel pathway of miR-134/CREB. Int J Clin Exp Pathol 8: 14472-14478, 2015.
35. Pan JY, Zhang F, Sun CC, Li SJ, Li G, Gong FY, Bo T, He J, Hua RX, Hu WD, *et al*: miR-134: A Human Cancer Suppressor? Mol Ther Nucleic Acids 6: 140-149, 2017.
36. Acunzo J, Roche C, Defilles C, Thirion S, Quentien MH, Figarella-Branger D, Graillon T, Dufour H, Brue T, Pellegrini I, *et al*: Inactivation of PITX2 transcription factor induced apoptosis of gonadotroph tumoral cells. Endocrinology 152: 3884-3892, 2011.
37. Hirose H, Ishii H, Mimori K, Tanaka F, Takemasa I, Mizushima T, Ikeda M, Yamamoto H, Sekimoto M, Doki Y, *et al*: The significance of PITX2 overexpression in human colorectal cancer. Ann Surg Oncol 18: 3005-3012, 2011.
38. Zhang JX, Chen ZH, Xu Y, Chen JW, Weng HW, Yun M, Zheng ZS, Chen C, Wu BL, Li EM, *et al*: Downregulation of MicroRNA-644a Promotes Esophageal Squamous Cell Carcinoma Aggressiveness and Stem Cell-like Phenotype via Dysregulation of PITX2. Clin Cancer Res 23: 298-310, 2017.